Double- β Decay

OMITTED FROM SUMMARY TABLE NEUTRINOLESS DOUBLE- β DECAY

Revised August 2019 by A. Piepke (University of Alabama) and P. Vogel (Caltech) .

Observation of neutrinoless double-beta $(0\nu\beta\beta)$ decay would signal violation of total lepton number conservation. The process can be mediated by an exchange of a light Majorana neutrino, or by an exchange of other particles. However, the existence of $0\nu\beta\beta$ -decay requires a nonvanishing Majorana neutrino mass, no matter what the actual mechanism is. As long as only a limit on the lifetime is available, limits on the effective Majorana neutrino mass, on the lepton-number violating righthanded current or other possible mechanisms mediating $0\nu\beta\beta$ decay can be obtained, independently of the actual mechanism, by assuming that one of these "new physics" possibilities dominates. These limits are listed in the Double- β Decay Listings of the experimental measurements.

In the following we assume that the exchange of light Majorana neutrinos $(m_{\nu_i} \leq 10 \text{ MeV})$ contributes dominantly to the decay rate. Besides a dependence on the phase space $(G^{0\nu})$ and the nuclear matrix element $(M^{0\nu})$, the observable $0\nu\beta\beta$ -decay rate is proportional then to the square of the effective Majorana mass m_{ee} , $(T_{1/2}^{0\nu})^{-1} = G^{0\nu} \cdot |M^{0\nu}|^2 \cdot m_{ee}^2$, with $m_{ee}^2 = |\sum_i U_{ei}^2 m_{\nu_i}|^2$. The sum contains, in general, complex CP-phases in U_{ei}^2 , i.e., cancellations may occur. For three neutrino flavors there are two physical phases for Majorana neutrinos (η_1, η_2) and one for Dirac neutrinos (δ_{CP}) . The relevant Majorana phases affect only processes to which lepton-number changing amplitudes contribute. Given the general 3×3 mixing matrix for Majorana neutrinos, one can construct

other analogous lepton number violating quantities, $m_{\ell\ell'} = \sum_i U_{\ell i} U_{\ell' i} m_{\nu_i} (\ell \text{ or } \ell' \neq e)$. However, these are currently much less constrained than m_{ee} .

Nuclear structure calculations are needed to deduce m_{ee} from the decay rate. While $G^{0\nu}$ can be calculated accurately, the computation of $M^{0\nu}$ is subject to uncertainty. Comparing different nuclear model evaluations indicates a factor \sim 2-3 spread in the calculated nuclear matrix elements. Nuclear structure calculation consistently overestimate Gamow-Teller (axial current) matrix elements. This inability of the nuclear models to reproduce Gamow-Teller decay rates is often parametrized in form of a modified coupling constant q_A . Many nuclear theorists interpret this shortcoming as evidence that important physics is missing in the modeling of weak nuclear transitions. It is not clear how these observed uncertainties impact $0\nu\beta\beta$ -matrix elements. Nevertheless, this constitutes an additional element of uncertainty. Recent work, 1 shows how the discrepancy between experimental and theoretical axial current matrix elements might be resolved. However, application of this approach to the $0\nu\beta\beta$ decay remains to be accomplished. The particle physics quantities to be determined are thus nuclear model-dependent, so the half-life measurements are listed first. Where possible, we reference the nuclear matrix elements used in the subsequent analysis. Since rates for the conventional $2\nu\beta\beta$ decay serve to constrain the nuclear theory models, results for this process are also given.

Oscillation experiments utilizing atmospheric, accelerator, solar, and reactor produced neutrinos and anti-neutrinos show that at least some neutrinos are massive. However, so far the inverted mass ordering (i.e., whether $\Delta m_{31}^2 < 0$) is disfavored only by 2-3 σ compared to the normal mass ordering (when

 $\Delta m_{31}^2 > 0$), while the absolute neutrino mass values or the properties of neutrinos under CPT-conjugation (Dirac or Majorana) remain undetermined. All confirmed oscillation experiments can be consistently described using three interacting neutrino species with two mass splittings and three mixing angles. (For values of the mixing angles and mass square differences see the corresponding tables.)

Based on the 3-neutrino analysis:

 $m_{ee}^2 = |\cos^2 \theta_{13} \cos^2 \theta_{12} m_1 + e^{2i(\eta_2 - \eta_1)} \cos^2 \theta_{13} \sin^2 \theta_{12} m_2 + e^{2i(\eta_2 - \eta_1)} \cos^2 \theta_{13} \sin^2 \theta_{12} m_2 + e^{2i(\eta_2 - \eta_1)} \cos^2 \theta_{13} \sin^2 \theta_{12} m_2 + e^{2i(\eta_2 - \eta_1)} \cos^2 \theta_{13} \sin^2 \theta_{12} m_2 + e^{2i(\eta_2 - \eta_1)} \cos^2 \theta_{13} \sin^2 \theta_{12} m_2 + e^{2i(\eta_2 - \eta_1)} \cos^2 \theta_{13} \sin^2 \theta_{12} m_2 + e^{2i(\eta_2 - \eta_1)} \cos^2 \theta_{13} \sin^2 \theta_{12} m_2 + e^{2i(\eta_2 - \eta_1)} \cos^2 \theta_{13} \sin^2 \theta_{12} m_2 + e^{2i(\eta_2 - \eta_1)} \cos^2 \theta_{13} \sin^2 \theta_{13} m_2 + e^{2i(\eta_2 - \eta_1)} \cos^2 \theta_{13} \sin^2 \theta_{13} m_2 + e^{2i(\eta_2 - \eta_1)} \cos^2 \theta_{13} m_2 + e^{2$ $e^{-2i(\eta_1+\delta_{CP})}\sin^2\theta_{13}m_3|^2$, valid for both mass orderings. Given the present knowledge of the neutrino oscillation parameters one can derive a relation between the effective Majorana mass and the mass of the lightest neutrino, as illustrated in Figure 14.11 in the Neutrino Masses, Mixing and Oscillations review. The three mass orderings allowed by the oscillation data: normal $(m_1 < m_2 \ll m_3)$, inverted $(m_3 \ll m_1 < m_2)$, and degenerate $(m_1 \approx m_2 \approx m_3)$, result in different projections. The width of the colored bands reflects the uncertainty introduced by the unknown Majorana and Dirac phases as well as the experimental errors of the oscillation parameters. The latter causes only minor broadening of the bands. Because of the overlap of the different mass scenarios, a measurement of m_{ee} would not reveal which mass ordering is applicable, provided the value of m_{ee} is in the overlapping range.

Analogous plots depict the relation of m_{ee} with the summed neutrino mass $m_{tot} = m_1 + m_2 + m_3$, constrained by observational cosmology, and m_{ee} as a function of the average mass $m_{\nu_e}^{eff} = [\Sigma |U_{ei}|^2 m_{\nu_i}^2]^{1/2}$ determined through the analysis of the electron energy distribution in low energy beta decays. (See Fig. 1 of [2].) The oscillation data thus allow to test whether observed values of m_{ee} and m_{tot} or $m_{\nu_e}^{eff}$ are consistent within

the 3 neutrino framework. The rather large intrinsic width of the $\beta\beta$ -decay constraints essentially does not allow to positively identify the mass ordering, and thus the sign of Δm_{31}^2 , even in combination with these other observables. Naturally, if a value of $0 < m_{ee} \leq 0.01$ eV is ever established, then the normal mass ordering becomes the only possible scenario.

It should be noted that systematic uncertainties of the nuclear matrix elements and possible quenching of the axial current matrix elements are sometimes not folded into the mass limits reported by $\beta\beta$ -decay experiments. Taking this additional uncertainty into account would further widen the projections. The plots are based on a 3-neutrino analysis. If it turns out that additional, i.e. sterile light neutrinos exist, the allowed regions would be modified substantially.

If neutrinoless double-beta decay is observed, it will be possible to fix a range of absolute values of the masses m_{ν_i} . Unlike the direct neutrino mass measurements, however, a limit on m_{ee} does not allow one to constrain the individual mass values m_{ν_i} even when the mass differences Δm_{ij}^2 are known.

Neutrino oscillation data imply the existence of a lower limit ~ 0.014 eV for the Majorana neutrino mass for the inverted mass ordering pattern, while m_{ee} could, by fine tuning, vanish in the case of the normal mass ordering. Several new doublebeta searches have been proposed to probe the interesting m_{ee} mass range, with the prospect of full coverage of the inverted mass ordering region within the next decade.

The $0\nu\beta\beta$ decay mechanism discussed so far is not the only way in which the decay can occur. Numerous other possible scenarios have been proposed, however, all of them requiring new physics. It will be a challenging task to decide which mechanism was responsible once $0\nu\beta\beta$ decay is observed. LHC experiments may reveal corresponding signatures for new

https://pdg.lbl.gov

Created: 5/31/2024 10:16

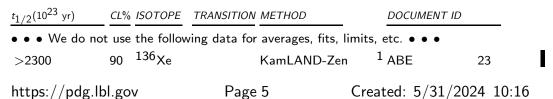
physics of lepton number violation. If lepton-number violating right-handed weak current interactions exist, its strength can be characterized by the phenomenological coupling constants η and λ (η describes the coupling between the right-handed lepton current and left-handed quark current while λ describes the coupling when both currents are right-handed). The $0\nu\beta\beta$ decay rate then depends on $\langle \eta \rangle = \eta \sum_{i} U_{ei} V_{ei}$ and $\langle \lambda \rangle = \lambda \sum_{i} U_{ei} V_{ei}$ that vanish for massless or unmixed neutrinos $(V_{\ell j})$ is a matrix analogous to $U_{\ell i}$ but describing the mixing with the hypothetical right-handed neutrinos). The observation of the single electron spectra could, in principle, allow to distinguish this mechanism of $0\nu\beta\beta$ from the light Majorana neutrino exchange driven mode. The limits on $\langle \eta \rangle$ and $\langle \lambda \rangle$ are listed in a separate table. The reader is cautioned that a number of earlier experiments did not distinguish between η and λ . In addition, see the section on Majoron searches for additional limits set by these experiments.

References

- P. Gysbers *et al.*, Nature Phys. **15**, 5 (2019); [arXiv:1903.00047].
- M.J. Dolinski, A.W.P. Poon and W. Rodejohann, Ann. Rev. Nucl. Part. Sci. 49, 219 (2019); [arXiv:1902.04097].

Half-life 0ν double- β decay

In most cases the transitions (Z,A) \rightarrow (Z+2,A) + 2e⁻ to the 0⁺ ground state of the final nucleus are listed. We also list transitions that decrease the nuclear charge (2e⁺, e⁺ CC and double EC) and transitions to an excited state of the final nucleus (0⁺_i, 2⁺, and 2⁺_i). In the following Listings only the best or comparable limits for the half-lives of each transition are reported and only those with about T_{1/2} > 10²³ years that are relevant for particle physics.



> 020	00	76 _{Ge}				00
> 830	90 00	100		MAJORANA	² ARNQUIST ³ AUGIER	23
> 2.1	90		g.s. $\rightarrow 2^+_1$			23
> 1.2	90	100 _{Mo}	g.s. $ ightarrow 0^+_1$	CUPID-Mo	³ AUGIER	23
> 13	90	¹³⁶ Xe		NEXT	⁴ NOVELLA	23
> 220	90	¹³⁰ Те ¹²⁸ Те		CUORE	⁵ ADAMS	22A
> 36	90	¹²⁰ Te 136Xe		CUORE	⁶ ADAMS	22B
> 12	90	100 Xe 100 Mo		XENON1T	⁷ APRILE	22A
> 18	90 00	⁸² Se		CUPID-Mo	⁸ AUGIER ⁹ AZZOLINI	22
> 46	90 00	⁸² Se	. o+	CUPID-0		22
> 1.8	90		g.s. $\rightarrow 0^+_1$		¹⁰ AZZOLINI	22
> 3.0	90	⁸² Se	g.s. $\rightarrow 2^+_1$		¹¹ AZZOLINI	22
> 3.2	90	82 _{Se}	g.s. $\rightarrow 2^+_2$		¹² AZZOLINI	22
> 59	90	¹³⁰ Te	g.s. $\rightarrow 0^+_1$	CUORE	¹³ ADAMS	21A
> 15	90	100_{Mo}	-	CUPID-Mo	¹⁴ ARMENGAUD	21
> 39.9	90	^{76}Ge	g.s. $\rightarrow 0^+_1$	MAJORANA-Dem	¹⁵ ARNQUIST	21
> 21.2	90	76 _{Ge}		MAJORANA-Dem	¹⁶ ARNQUIST	21
> 9.7	90	^{76}Ge	g.s. $\rightarrow 2^+_2$	MAJORANA-Dem	¹⁷ ARNQUIST	21
> 320	90	¹³⁰ Te	2	CUORE	¹⁸ ADAMS	20A
>1800	90	^{76}Ge		GERDA	¹⁹ AGOSTINI	20 B
> 14	90	¹³⁰ Te	g.s. $\rightarrow 0^+_1$	CUORE-0	²⁰ ALDUINO	19
> 0.95	90	100 _{Mo}	T	AMoRE	²¹ ALENKOV	19
> 350	90	¹³⁶ Xe		EXO-200	²² ANTON	19
> 2.4	90	^{136}Xe		PANDAX-II	²³ NI	19
> 150	90	¹³⁰ Te		CUORE	²⁴ ALDUINO	18
> 2.5	90	⁸² Se		NEMO-3	²⁵ ARNOLD	18
> 2.2	90	¹¹⁶ Cd		AURORA	²⁶ BARABASH	18
> 1.1	90	¹³⁴ Xe		EXO-200	²⁷ ALBERT	17C
> 1	90	¹¹⁶ Cd		NEMO-3	²⁸ ARNOLD	17
> 40	90	¹³⁰ Te		CUORICINO	²⁹ ALDUINO	16
> 260	90		$g.s. \rightarrow 2^+_1$	KamLAND-Zen	³⁰ ASAKURA	16
> 260	90		$g.s. \rightarrow 2^+_2$	KamLAND-Zen	³¹ ASAKURA	16
> 240	90	¹³⁶ Xe	$g.s.\!\to 0_1^+$	KamLAND-Zen	³² ASAKURA	16
> 11	90	¹⁰⁰ Mo		NEMO-3	³³ ARNOLD	15
> 9.4	90	¹³⁰ Te	g.s. $\rightarrow 0^+_1$	CUORICINO	³⁴ ANDREOTTI	12
> 0.58	90	⁴⁸ Ca	1	CaF ₂ scint.	³⁵ UMEHARA	08
> 0.89	90	100 _{Mo}	g.s. $\rightarrow 0^+_1$		³⁶ ARNOLD	07
> 1.6	90	100 _{Mo}	g.s. $\rightarrow 2^+$		³⁷ ARNOLD	07
> 1.1	90	¹²⁸ Te	-	Cryog. det.	³⁸ ARNABOLDI	03
> 1.7	90	^{116}Cd		¹¹⁶ CdWO ₄ scint.	³⁹ DANEVICH	03
> 157	90	76 _{Ge}		Enriched HPGe	⁴⁰ AALSETH	0 2B
_						

¹ABE 23 use the combined data set of the KamLAND-Zen 400 and 800 experiments, utilizing 745 kg of isotopically enriched xenon (90.9% ¹³⁶Xe), dissolved in liquid scintillator and an exposure of 970 kg·yr of ¹³⁶Xe, to derive this limit on $0\nu\beta\beta$ decay. A half-life sensitivity of 1.5×10^{26} yr is reported.

- ² ARNQUIST 23 use the final data set of the MAJORANA DEMONSTRATOR experiment, operating enriched in ⁷⁶Ge detectors, to set this limit on the $0\nu\beta\beta$ half-life of ⁷⁶Ge. The exposure is 64.5 kg·yr. A median sensitivity of 8.1×10^{25} yr is reported.
- ³ AUGIER 23 utilize the complete data, set collected by the CUPID-Mo bolometric calorimeter with particle ID and located at the LSM, to study various double beta decays of 100 Mo to excited states of the daughter nucleus. An exposure of 1.47 kg·yr of 100 Mo is available.
- ⁴ NOVELLA 23 use data collected by the NEXT-White experiment to limit the 0 $\nu \beta \beta$ half-life of ¹³⁶Xe. The experiment contains 3.5 kg of enriched Xe and is based on a high-pressure gas TPC. Two different limits are reported, based on different data analysis approaches, $> 5.5 \times 10^{23}$ yr and $> 13 \times 10^{23}$ yr.
- ⁵ ADAMS 22A use the CUORE TeO₂ experiment with an exposure of 288.8 kg·yr of ¹³⁰Te to place a limit on its $0\nu \beta\beta$ decay. The median sensitivity is reported as 280×10^{23} yr. Superseeds ADAMS 20A.
- ⁶ ADAMS 22B use the CUORE bolometric calorimeter to place a limit on the $0\nu\beta\beta$ decay half-life of ¹²⁸Te.
- $^7\,\rm APRILE~22A$ use 36.16 kg·yr of $^{136}\rm Xe$ exposure of the XENON1T not enriched detector to establish the stated limit.
- ⁸ AUGIER 22 use the final data set of the CUPID-Mo cryogenic calorimeter, utilizing enriched Li₂¹⁰⁰ MoO₄ and an isotope exposure of 1.47 kg·y, to place a limit on the $0\nu\beta\beta$ decay half-life.
- ⁹ AZZOLINI 22 use the CUPID-0 scintillating cryogenic bolometer to set a limit on the $0\nu\beta\beta$ half-life of ⁸²Se. The analyzed isotope exposure is 8.82 kg·yr. A median sensitivity of 7×10^{24} yr is reported. Supersedes AZZOLINI 19.
- ¹⁰ AZZOLINI 22 use CUPID-0 data with an isotope exposure of 8.82 kg·yr to set a limit on the $0\nu\beta\beta$ decay to the first excited 0^+ state.
- ¹¹ AZZOLINI 22 use CUPID-0 data with an isotope exposure of 8.82 kg·yr to set a limit on the $0\nu\beta\beta$ decay to the first excited 2⁺ state.
- ¹² AZZOLINI 22 use CUPID-0 data with an isotope exposure of 8.82 kg·yr to set a limit on the $0\nu\beta\beta$ decay to the second excited 2⁺ state.
- 13 ADAMS 21A et al. used 101.76 kg yr of 130 Te exposure of the CUORE (LNGS) bolometric detector to place a limit on the decay to the first excited state of 130 Xe, superseding ALDUINO 19 as the most restrictive bound on this particular decay.
- 14 ARMENGAUD 21 use the CUPID-Mo 4.2 kg array of enriched ${\rm Li_2}^{100}{\rm MoO_4}$ scintillating bolometers, with 1.17 kg·yr exposure, to set this limit.
- 15 ARNQUIST 21 use the MAJORANA demonstrator to set this limit for the 0 ν $\beta\beta$ decay to the first excited 0⁺ state, with a 41.9 kg yr isotopic exposure. The median sensitivity is 39.9 \times 10²³ yr.
- 16 ARNQUIST 21 use the MAJORANA demonstrator to set this limit for the 0 ν $\beta\beta$ decay to the first excited 2⁺ state, with a 41.9 kg yr isotopic exposure. The median sensitivity is 21.2 \times 10²³ yr.
- 17 ARNQUIST 21 use the MAJORANA demonstrator to set this limit for the 0 ν β β decay to the second excited 2⁺ state, with a 41.9 kg yr isotopic exposure. The median sensitivity is 18.6 \times 10²³ yr.
- 18 ADAMS 20A use the CUORE detector to search for the 0ν $\beta\beta$ decay of 130 Te. The exposure was 372.5 kg·yr of TeO_2 corresponding to 103.6 kg·yr of 130 Te. The exclusion sensitivity is 1.7×10^{25} yr. Supersedes ALDUINO 18.
- ¹⁹ AGOSTINI 20B present the final data set of the GERDA experiment, searching for $0\nu \beta\beta$ decay of ⁷⁶Ge with isotopically enriched, high resolution Ge detectors. A final exposure of 127.2 kg·yr is reported. The experiment reports the lowest background and longest half life limit ever achieved by any double beta decay experiment. The reported experiment sensitivity equals the limit. Supersedes AGOSTINI 19.

- ²⁰ ALDUINO 19 use the combined data of the CUORICINO and CUORE-0 experiments to place a lower limit on the half life of the $0\nu \beta\beta$ decay of ¹³⁰Te to the first excited 0⁺ state of ¹³⁰Xe. Supersedes ANDREOTTI 12.
- ²¹ ALENKOV 19 report the 0 ν $\beta\beta$ decay half-life limit based on the 52.1 kg d exposure of ¹⁰⁰Mo, of a a cryogenic dual heat and light detector in the Yangyang underground laboratory. The median sensitivity is 1.1×10^{23} years.
- 22 ANTON 19 uses he complete dataset of the EXO-200 detector to search for the 0 ν $\beta\beta$ decay. The exposure is 234.1 kg yr. The median sensitivity is 5.0 \times 10 25 yr. Supersedes a ALBERT 18 and ALBERT 14B.
- ^{ALBERT 16 and ALBERT 14B.} ²³ NI 19 use the PandaX-II dual phase TPC at CJPL to search for the $0\nu \beta\beta$ decay of 136 Xe. The half-life limit 2.4 × 10^{23} yr is obtained from 22.2 kg yr exposure with a sensitivity of 1.9×10^{23} yr.
- ²⁴ ALDUINO 18 uses the CUORE detector to search for the 0 ν $\beta\beta$ decay of ¹³⁰Te. The exposure is 86.3 kg·year of natural TeO₂ corresponding to 24.0 kg·year for ¹³⁰Te. The median sensitivity is 0.7 × 10²⁵ yr. The limit is obtained combining the new data from CUORE with those of CUOREO (9.8 kg·year of ¹³⁰Te) and Cuoricino (19.8 kg·year of ¹³⁰Te).
- 25 ARNOLD 18 use the NEMO-3 tracking detector to place a limit on the $0\nu\beta\beta$ decay of 82 Se. This is a slightly weaker limit than in BARABASH 11A, using the same detector. Supersedes ARNOLD 05A.
- ²⁶ BARABASH 18 use 1.162 kg of ¹¹⁶CdWO₄ scintillating crystals to obtain this limit. Supersedes DANEVICH 03 with analogous source and is more sensitive than ARNOLD 17.
- 27 ALBERT 17C uses the EXO-200 detector that contains 19.098 \pm 0.014% admixture of 134 Xe to search for the 0 ν and 2 ν $\beta\beta$ decay modes. The exposure is 29.6 kg·year. The median sensitivity is 1.9×10^{21} years.
- ²⁸ ARNOLD 17 use the NEMO-3 tracking calorimeter, containing 410 g of enriched ¹¹⁶Cd exposed for 5.26 yr, to determine the half-life limit. Supersedes BARABASH 11A.
- ²⁹ ALDUINO 16 report result obtained with 9.8 kg y of data collected with the CUORE-0 bolometer, combined with data from the CUORICINO. Supersedes ALFONSO 15.
- ³⁰ASAKURA 16 use the KamLAND-Zen liquid scintillator calorimeter (¹³⁶Xe 89.5 kg yr) to place a limit on the $0\nu\beta\beta$ -decay into the first excited state of the daughter nuclide.
- ³¹ASAKURA 16 use the KamLAND-Zen liquid scintillator calorimeter (¹³⁶Xe 89.5 kg yr) to place a limit on the $0\nu\beta\beta$ -decay into the second excited state of the daughter nuclide.
- ³²ASAKURA 16 use the KamLAND-Zen liquid scintillator calorimeter (¹³⁶Xe 89.5 kg yr) to place a limit on the $0\nu\beta\beta$ -decay into the third excited state of the daughter nuclide.
- ³³ ARNOLD 15 use the NEMO-3 tracking calorimeter with 34.3 kg yr exposure to determine the limit of $0\nu\beta\beta$ -half life of ¹⁰⁰Mo. Supersedes ARNOLD 2005A and BARABASH 11A.
- ³⁴ ANDREOTTI 12 use high resolution TeO₂ bolometric calorimeter to search for the $0\nu\beta\beta$ decay of ¹³⁰ Te leading to the excited 0^{1}_{\perp} state at 1793.5 keV.
- 35 UMEHARA 08 use CaF₂ scintillation calorimeter to search for double beta decay of 48 Ca. Limit is significantly more stringent than quoted sensitivity: 18×10^{21} years.
- ³⁶Limit on 0 ν -decay to the first excited 0⁺₁-state of daughter nucleus using NEMO-3 tracking calorimeter. Supersedes DASSIE 95.
- 37 Limit on 0 ν -decay to the first excited 2⁺-state of daughter nucleus using NEMO-3 tracking calorimeter.
- ³⁸Supersedes ALESSANDRELLO 00. Array of TeO₂ crystals in high resolution cryogenic calorimeter. Some enriched in ¹²⁸Te. Ground state to ground state decay.
- 39 Limit on $0\nu\beta\beta$ decay of 116 Cd using enriched CdWO_4 scintillators. Supersedes a DANEVICH 00.
- ⁴⁰ AALSETH 02B limit is based on 117 mol·yr of data using enriched Ge detectors. Background reduction by means of pulse shape analysis is applied to part

of the data set. Reported limit is slightly less restrictive than that in KLAPDOR-KLEINGROTHAUS 01 However, it excludes part of the allowed half-life range reported in KLAPDOR-KLEINGROTHAUS 01B for the same nuclide. The analysis has been criticized in KLAPDOR-KLEINGROTHAUS 04B. The criticism was addressed and disputed in AALSETH 04.

Half-life measurements of the two-neutrino double- β decay

The measured half-life values for the transitions (Z,A) \rightarrow (Z+2,A) + 2 e^- + 2 $\overline{\nu}_e$ to the 0⁺ ground state of the final nucleus are listed. We also list the transitions to an excited state of the final nucleus (0⁺_i, etc.). We report only the measuremetnts with the smallest (or comparable) uncertainty for each transition.

$t_{1/2}(10^{20} \text{ yr})$)				ISOTOPE	TRANSITIO	NMETHOD		DOCUMENT ID	
• • • We	do r	not use t	the	followin	g data f	or averages	s, fits, limits, e	tc.	• • •	
20.22	\pm	0.18	±	0.38	^{76}Ge		GERDA	1	AGOSTINI	23
1.11	+ -	0.19 0.14	—	0.17 0.15	¹⁵⁰ Nd	$0^+ \rightarrow 0^+_1$	NEMO-3	2	AGUERRE	23
7.5	±	0.8	+	0.4 0.3			CUPID-Mo	3	AUGIER	23
0.0707	$7\pm$	0.0002		0.0011	¹⁰⁰ Mo		CUPID-Mo	4	AUGIER	23A
0.869	±	0.005	_	0.009 0.006	⁸² Se		CUPID-0	5	AZZOLINI	23A
21.6	+	6.2 4.0	+	4.0 2.9	¹³⁶ Xe		NEXT	6	NOVELLA	23
21900	± 7	00			¹²⁸ Te		CUORE		ADAMS	22в
110	\pm	20	± 1	LO	¹²⁴ Xe		XENON1T		APRILE	22A
118	±	13	± 1	L4	¹²⁴ Xe		XENONnT	9	APRILE	22B
23.4	+ -	0.8 4.6	$^+$	3.0 1.7	¹³⁶ Xe		NEXT	10	NOVELLA	22
8.76	+	0.09 0.07	+	0.14 0.17	130 Te		CUORE	11	ADAMS	21
180	±	50	±1	LO	¹²⁴ Xe	$2\nu \text{DEC}$	XENON1T	12	APRILE	19E
0.0680	0±	0.0001	+	0.0038 0.0040	¹⁰⁰ Mo		NEMO-3	13	ARNOLD	19
0.939	\pm	0.017			⁸² Se		NEMO-3	14	ARNOLD	18
0.263	+	$0.011 \\ 0.012$			^{116}Cd		AURORA	15	BARABASH	18
> 0.87					¹³⁴ Xe		EXO-200	16	ALBERT	17C
8.2	±	0.2	\pm	0.6	¹³⁰ Te		CUORE-0		ALDUINO	17
0.274	\pm	0.004	\pm	0.018	116 Cd		NEMO-3	18	ARNOLD	17
0.64	+	0.07 0.06	_	0.12 0.09	⁴⁸ Ca		NEMO-3	19	ARNOLD	16
0.0934	$4\pm$	0.0022	2+	$\begin{array}{c} 0.0062 \\ 0.0060 \end{array}$	¹⁵⁰ Nd		NEMO-3	20	ARNOLD	16A
19.26	±	0.94			76 _{Ge}		GERDA		AGOSTINI	15A
0.0693	$3\pm$	0.0004	ŀ		100_{Mo}		NEMO-3		ARNOLD	15
21.65	\pm	0.16	\pm	0.59	¹³⁶ Xe		EXO-200	23	ALBERT	14
92	+	55 26	±	13	⁷⁸ Kr		BAKSAN	24	GAVRILYAK	13
23.8	\pm	0.2	±	1.4	¹³⁶ Xe		KamLAND-Z			12A
7.0	\pm	0.9	\pm	1.1	¹³⁰ Te		NEMO-3		ARNOLD	11
0.235	\pm	0.014	\pm	0.016	⁹⁶ Zr		NEMO-3	27	ARGYRIADES	10

6.9	+	1.0 0.8	\pm 0.7	100 Mo 0 $^+ ightarrow 0_1^-$	⁺ Ge coinc.	²⁸ BELLI	10
5.7	+	1.3 0.9	\pm 0.8	100 Mo 0 $^+$ $ ightarrow$ 0 $^+_1$	NEMO-3	²⁹ ARNOLD	07
0.96	\pm	0.03	\pm 0.10	⁸² Se	NEMO-3	³⁰ ARNOLD	05A
0.29	+	0.04 0.03		¹¹⁶ Cd	CdWO ₄ sc.	³¹ DANEVICH	03

¹ AGOSTINI 23 report an updated value for the $2\nu \ \beta \beta$ half-life of ⁷⁶Ge; the final result of the GERDA Phase II experiment. A subset of the data, corresponding to an exposure of exposure is 11.8 kg·yr, is utilized. This is one of the most precise measurements of $2\nu \ \beta \beta$ decay reported in the literature. An effective nuclear matrix element of 0.101 ± 0.001 is derived from this result.

²AGUERRE 23 report the results of a 5.25 yr search for the $2\nu \beta\beta$ decay to the exited $0^+ \rightarrow 0^+_1$ state of the daughter nucleus, using the NEMO-3 tracking calorimeter. 36.6g of ¹⁵⁰Nd isotope were available for the measurement of this decay rate.

³AUGIER 23 utilize the complete data, set collected by the CUPID-Mo bolometric calorimeter with particle ID and located at the LSM, to measure the ¹⁰⁰Mo $2\nu\beta\beta$ half-life to excited 0_1^+ state of the daughter nucleus. An exposure of 1.47 kg·yr of ¹⁰⁰Mo is available.

⁴ AUGIER 23A use full data set collected by the CUPID-Mo experiment to derive an improved $2\nu \ \beta \beta$ g.s. to g.s. half-life of ¹⁰⁰Mo. An exposure of 1.48 kg·yr of ¹⁰⁰Mo is utilized. Supersedes ARMENGAUD 20.

⁵ AZZOLINI 23A report an improved measurement of the $2\nu \beta\beta$ decay with an exposure of 8.82 kg·yr of ⁸²Se, collected with the CUPID-0 detector. Superseded AZZOLINI 19B.

⁶ NOVELLA 23 used the NEXT-White experiment, with a fiducial mass of 3.5 kg of enriched xenon, to measure the $2\nu \beta\beta$ g.s. to g.s. half-life of ¹³⁶Xe. The experiment is based on a high-pressure gas TPC. Supersedes NOVELLA 22.

⁷ ADAMS 22B derive the $2\nu\beta\beta$ half-life of ¹²⁸Te from data of the CUORE bolometric calorimeter and the half-live ratio for ¹³⁰Te / ¹²⁸Te reported in BERNATOWICZ 92.

⁸ APRILE 22A report an improved ¹²⁴Xe 2νDEC half-life measurement for ¹²⁴Xe, using data collected by the XENON1T detector with an isotopically not enriched Xe target. The analyzed ¹²⁴Xe exposure is 0.87 kg·yr. The statistical significance of the signal is 7.0 sigma. The stated half-life considers captures from the K shell up to the N5 shell. This result supersedes APRILE 19E, which exclusively considered captures from the K shell.

 9 APRILE 22B use data collected by the XENONnT dark matter experiment to derive an improved $^{124} \rm Xe~2\nu DEC$ half-life measurement for $^{124} \rm Xe$. This result supersedes APRILE 22A.

¹⁰ NOVELLA 22 report on a high-pressure gas TPC at Canfranc underground laboratory, filled with 3.5 kg (fiducial) xenon gas, used to measure the $2\nu \beta\beta$ decay of ¹³⁶Xe. Topological track reconstruction is utilized in the data analysis. The measurement is based on comparing runs with isotopically enriched and depleted xenon. Other measurements with smaller error exist.

¹¹ ADAMS 21 use 102.7 kg yr of ¹³⁰Te exposure, collected by the CUORE bolometric detector at LNGS, to perform a measurement of the $2\nu \beta\beta$ decay of ¹³⁰Te. The dataset is more than 10-times that collected by the CUORE-0 experiment. The result has been revised in ADAMS 23A. Supersedes ALDUINO 17.

¹² APRILE 19E report first measurement of two-neutrino double electron capture in ¹²⁴Xe using the XENON1T detector with a 0.73 t-yr exposure. An excess of 126 \pm 29 events is observed at 64.3 \pm 0.6 keV decay energy, corresponding to $\sqrt{\Delta\chi^2} = 4.4$ with respect to the background-only hypothesis.

¹³ ARNOLD 19 use the NEMO-3 tracking calorimeter with 34.3 kg y exposure to determine the $2\nu \beta\beta$ half-life of ¹⁰⁰Mo. Supersedes ARNOLD 15.

- ¹⁴ ARNOLD 18 use the NEMO-3 tracking detector to determine the $2\nu\beta\beta$ half-life of ⁸²Se. 0.93 kg of 82 Se was observed for 5.25 y. The half-life value was obtained based on the single-state-dominance (SSD) hypothesis, preferred in this case by about 2 σ . Supersedes
- ARNOLD 05A. ¹⁵ BARABASH 18 use 1.162 kg of ¹¹⁶CdWO₄ scintillating crystals to obtain this value. Supersedes DANEVICH 03 with analogous source and agrees with ARNOLD 17 with the NEMO-3 detector.
- $^{16}\,\text{ALBERT}$ 17C uses the EXO-200 detector that contains 19.098 \pm 0.014% admixture of 134 Xe to search for the 2ν $\beta\beta$ decay mode. The exposure is 29.6 kg·year. The median sensitivity is 1.2×10^{21} years.
- 17 ALDUINO 17 use the CUORE-0 detector containing 10.8 kg of 130 Te in 52 crystals of TeO₂. The exposure was 9.3 kg yr of 130 Te. This is a more accurate rate determination than in ARNOLD 11 and BARABASH 11A. ¹⁸ ARNOLD 17 use the NEMO-3 tracking calorimeter, containing 410 grams of enriched
- 116 Cd exposed for 5.26 years, to determine the half-life value.
- 19 ARNOLD 16 use the NEMO-3 detector and a source of 6.99 g of 48 Ca. The half-life is based on 36.7 g year exposure. It is consistent, although somewhat longer, than the previous determinations of the half-life. Supersedes BARABASH 11A.
- 20 ARNOLD 16A use the NEMO-3 tracking calorimeter, containing 36.6 g of 150 Nd exposed for 1918.5 days, to determine the half-life. Supersedes ARGYRIADES 09.
- 21 AGOSTINI 15A use 17.9 kg yr exposure of the GERDA calorimeter to derive an improved measurement of the $2\nu\beta\beta$ decay half life of ⁷⁶Ge.
- ²² ARNOLD 15 use the NEMO-3 tracking calorimeter with 34.3 kg yr exposure to determine the $2\nu\beta\beta$ -half life of ¹⁰⁰Mo. Supersedes ARNOLD 05A and ARNOLD 04.
- 23 ALBERT 14 use the EXO-200 tracking detector for a re-measurement of the 2
 uetaeta-half life of 136 Xe. A nuclear matrix element of 0.0218 ± 0.0003 MeV $^{-1}$ is derived from this data. Supersedes ACKERMAN 11.
- 24 GAVRILYAK 13 use a proportional counter filled with Kr gas to search for the $2\nu 2$ K decay of ⁷⁸Kr. Data with the enriched and depleted Kr were used to determine signal and background. A 2.5 σ excess of events obtained with the enriched sample is interpreted as an indication for the presence of this decay.
- $^{25}\,{\sf GANDO}$ 12A use a modification of the existing KamLAND detector. The $\beta\beta$ decay source/detector is 13 tons of enriched ¹³⁶Xe-loaded scintillator contained in an inner balloon. The $2\nu\beta\beta$ decay rate is derived from the fit to the spectrum between 0.5 and 4.8 MeV. This result is in agreement with ACKERMAN 11.
- 26 ARNOLD 11 use enriched $^{\bar{130}}$ Te in the NEMO-3 detector to measure the 2u $\beta\beta$ decay rate. This result is in agreement with, but more accurate than ARNABOLDI 03.
- ²⁷ ARGYRIADES 10 use 9.4 \pm 0.2 g of ⁹⁶Zr in NEMO-3 detector and identify its $2\nu\beta\beta$ decay. The result is in agreement and supersedes ARNOLD 99.
- ²⁸ BELLI 10 use enriched ¹⁰⁰Mo with 4 HP Ge detectors to record the 590.8 and 539.5 keV γ rays from the decay of the 0⁺₁ state in ¹⁰⁰Ru both in singles and coincidences. This result confirms the measurement of KIDD 09 and ARNOLD 07 and supersedes them.
- ²⁹ First exclusive measurement of 2ν -decay to the first excited 0_1^+ -state of daughter nucleus. ARNOLD 07 use the NEMO-3 tracking calorimeter to detect all particles emitted in decay. Result agrees with the inclusive $(0\nu + 2\nu)$ measurement of DEBRAECKELEER 01.
- 30 ARNOLD 05A use the NEMO-3 tracking detector to determine the 2
 uetaeta half-life of 82 Se with high statistics and low background (389 days of data taking). Supersedes ARNOLD 04.
- ³¹DANEVICH 03 is calorimetric measurement of $2\nu\beta\beta$ ground state decay of ¹¹⁶Cd using enrichedCdWO₄ scintillators. Agrees with EJIRI 95 and ARNOLD 96. Supersedes DANEVICH 00.

$\langle m_{\rm ee} \rangle$, The Effective Weighted Sum of Majorana Neutrino Masses Contributing to Neutrinoless Double- β Decay

 $\langle m_{\rm ee}\rangle = |\Sigma U_{ei}^2 m_{\nu_i}|, i = 1,2,3.$ It is assumed that ν_i are Majorana particles and that the transition is dominated by the known (light) neutrinos. Note that U_{ei}^2 and not $|U_{ei}|^2$ occur in the sum, and that consequently cancellations are possible. The experiments obtain the limits on $\langle m_{\nu}\rangle$ from the measured ones on $T_{1/2}$ using a range of nuclear matrix elements (NME), which is reflected in the spread of $\langle m_{\nu}\rangle$. Different experiments may choose different NME. All assume $g_A = 1.27$. In the following Listings, only the best or comparable limits for each isotope are reported. When not mentioned explicitly the transition is between ground states, but transitions between excited states are also reported.

VALUE (eV)	ISOTOPE	METHOD	DOCUMENT ID	
$\bullet \bullet \bullet$ We do not use the	following	data for averages, fits	s, limits, etc. • • •	
< 0.036-0.156	¹³⁶ Xe	KamLAND-Zen	1 ABE	23
< 0.113-0.269	^{76}Ge	MAJORANA	² ARNQUIST	23
< 0.48–3.19	¹³⁶ Xe	NEXT	³ NOVELLA	23
< 0.09–0.305	¹³⁰ Te	CUORE	⁴ ADAMS	22A
< 0.8–2.5	136 Xe	XENON1T	⁵ APRILE	22A
< 0.28–0.49	¹⁰⁰ Mo	CUPID-Mo	⁶ AUGIER	22
< 0.263–0.545	⁸² Se	CUPID-0	⁷ AZZOLINI	22
< 0.31–0.54	¹⁰⁰ Mo	CUPID-Mo	⁸ ARMENGAUD	21
< 0.075–0.35	¹³⁰ Te	CUORE	⁹ ADAMS	20A
< 0.079-0.180	^{76}Ge	GERDA	¹⁰ AGOSTINI	20 B
< 1.2–2.1	¹⁰⁰ Mo	AMoRE	11 ALENKOV	19
< 0.093-0.286	¹³⁶ Xe	EXO-200	¹² ANTON	19
< 1.3–3.5	¹³⁶ Xe	PANDAX-II	¹³ NI	19
< 0.11–0.52	¹³⁰ Te	CUORE	¹⁴ ALDUINO	18
< 1.2–3.0	⁸² Se	NEMO-3	¹⁵ ARNOLD	18
< 1.0 - 1.7	¹¹⁶ Cd	AURORA	¹⁶ BARABASH	18
< 1.4–2.5	^{116}Cd	NEMO-3	¹⁷ ARNOLD	17
< 0.27–0.76	¹³⁰ Te	CUORICINO	¹⁸ ALDUINO	16
< 1.6–5.3	¹⁵⁰ Nd	NEMO-3	¹⁹ ARNOLD	16A
< 0.33–0.62	¹⁰⁰ Mo	NEMO-3	²⁰ ARNOLD	15
< 7.2–19.5	⁹⁶ Zr	NEMO-3	²¹ ARGYRIADES	10
< 3.5–22	⁴⁸ Ca	CaF ₂ scint.	²² UMEHARA	08
< 1.5 - 1.7	116 Cd	¹¹⁶ CdWO ₄ scint.	²³ DANEVICH	03

¹ABE 23 utilize 745 kg of ¹³⁶Xe isotope exposure from the combined data set of the KamLAND-Zen 400 and 800 to derive a limit on $\langle m_{\beta\beta} \rangle$. The range reflects the author's assessment of the variability of the theoretically calculated nuclear matrix elements.

² ARNQUIST 23 use the final data set of the MAJORANA DEMONSTRATOR experiment, with 64.5 kg·yr of isotop exposure, to derive an upper limit for $\langle m_{\beta\beta} \rangle$. The range reflects the author's assessment of the variability of the theoretically calculated nuclear matrix elements.

³NOVELLA 23 use data collected with the NEXT-White experiment to derive a range of upper limits for $\langle m_{\beta\beta} \rangle$. The range reflects the author's assessment of the variability of the theoretically calculated nuclear matrix elements and both half-life limits stated in NOVELLA 23.

- ⁴ ADAMS 22A use 1038.4 kg·yr of TeO₂ exposure collected by the CUORE experiment to determine this range of limits. The range reflects the uncertainty of nuclear matrix _ element calculations needed for the conversion of half-life to neutrino mass.
- ⁵ APRILE 22A use data taken with the XENON1T detector to limit the Majorana neutrino mass. 36.16 kg·yr of ¹³⁶Xe exposure were utilized. The reported range of limits is due to uncertainties in the nuclear matrix elements.
- ⁶ AUGIER 22 use the final data set of the CUPID-Mo cryogenic calorimeter with an isotop exposure of 1.47 kg·y to derive a range of neutrino mass limits. The range reflects the authors' estimate of the spread of nuclear matrix element calculations.
- ⁷ AZZOLINI 22 use 8.82 kg·yr of isotopic exposure of the CPID-0 scintillating cryogenic bolometer to set this range of neutrino mass limits. The range reflects the authors' estimate of the spread of nuclear matrix element calculations.
- ⁸ ARMENGAUD 21 use the CUPID-Mo demonstrator, with 1.17 kg·yr exposure of ¹⁰⁰Mo, to set this limit. The range reflects the estimated uncertainty of the calculated nuclear matrix elements.
- ⁹ADAMS 20A use the data of CUORE (372.5 kg·yr exposure of TeO₂) to obtain this limit.
- ¹⁰ AGOSTINI 20B use the final data set of the GERDA experiment, representing an exposure of 127.2 kg·yr to derive an upper limit for $\langle m_{\beta\beta} \rangle$. Isotopically enriched Ge detectors were used. The range reflects the variability of the theoretically calculated nuclear matrix elements. Supersedes AGOSTINI 19.
- $^{11}{}$ ALENKOV 19 report the range of the effective masses $\langle m_{\beta\,\beta}\rangle$ corresponding to the 0 ν

 $\beta\beta$ decay half-life limit. It is based on the 52.1 kg·d exposure of 100 Mo, in the Yangyang underground laboratory. The median sensitivity is 1.1×10^{23} years. The range of $\langle m_{\beta\beta}\rangle$ reflects the uncertainty of nuclear matrix elements.

- ¹² ANTON 19 uses the complete dataset of the EXO-200 experiment to obtain these limits. The spread reflect the uncertainty in the nuclear matrix elements. Supersedes ALBERT 18 and ALBERT 14B.
- ¹³ NI 19 use the PandaX-II dual phase TPC at CJPL to search for the $0\nu \beta\beta$ decay of ¹³⁶Xe with 22.2 kg yr exposure. The range in the $m_{\beta\beta}$ limit of 1.3–3.5 eV reflects the
- range of the calculated nuclear matrix elements. The sensitivity is $1.9 imes 10^{23}$ yr.
- ¹⁴ ALDUINO 18 use the combined data of CUORE, CUORE0, and Cuoricino to obtain this limit.
- ¹⁵ ARNOLD 18 use the NEMO-3 tracking detector to constrain the $0\nu\beta\beta$ decay of ⁸²Se. The limit on $\langle m_{\beta\beta} \rangle$ is obtained assuming light neutrino exchange; the range reflects different calculations of the nuclear matrix elements. This is a somewhat weaker limit than in BARABASH 11A using the same detector.
- 16 BARABASH 18 use 1.162 kg of 116 CdWO₄ scintillating crystals to obtain these limits. The spread reflects the estimated uncertainty in the nuclear matrix element. Supersedes DANEVICH 03.
- ¹⁷ ARNOLD 17 utilize NEMO-3 data, taken with enriched ¹¹⁶Cd to limit the effective Majorana neutrino mass. The reported range results from the use of different nuclear matrix elements. Supersedes BARABASH 11A.
- ¹⁸ ALDUINO 16 place a limit on the effective Majorana neutrino mass using the combined data of the CUORE-0 and CUORICINO experiments. The range reflects the authors' evaluation of the variability of the nuclear matrix elements. Supersededs ALFONSO 15.
- ¹⁹ ARNOLD 16A limit is derived from data taken with the NEMO-3 detector and ¹⁵⁰Nd. A range of nuclear matrix elements that include the effect of nuclear deformation have been used. Supersedes ARGYRIADES 09.
- 20 ARNOLD 15 use the NEMO-3 tracking calorimeter with 34.3 kg yr exposure to determine the neutrino mass limit based on the $0\nu\beta\beta$ -half life of 100 Mo. The spread range reflects different nuclear matrix elements. Supersedes ARNOLD 14 and BARABASH 11A.
- ²¹ ARGYRIADES 10 use ⁹⁶Zr and the NEMO-3 tracking detector to obtain the reported mass limit. The range reflects the fluctuation of the nuclear matrix elements considered.

- ²² Limit was obtained using CaF₂ scintillation calorimeter to search for double beta decay of ⁴⁸Ca. Reported range of limits reflects spread of QRPA and SM matrix element calculations used. Supersedes OGAWA 04.
- 23 Limit for $\langle m_{\nu}\rangle$ is based on the nuclear matrix elements of STAUDT 90 and ARNOLD 96. Supersedes DANEVICH 00.

Limits on Lepton-Number Violating (V+A) Current Admixture

For reasons given in the discussion at the beginning of this section, we list only results from 1989 and later. $\langle \lambda \rangle = \lambda \sum U_{ej} V_{ej}$ and $\langle \eta \rangle = \eta \sum U_{ej} V_{ej}$, where the sum is over the number of neutrino generations. This sum vanishes for massless or unmixed neutrinos. In the following Listings, only best or comparable limits or lifetimes for each isotope are reported.

$\left<\lambda\right>$ (10 ⁻⁶)	CL%	$\left<\eta\right>$ (10 ⁻⁸)	CL%	ISOTOPE	METHOD	DOCUMENT ID	
• • • We do	o not	use the followi	ng da	ata for aver	ages, fits, limits, et	C. ● ● ●	
< 2.2–2.6	90	< 1.7–2.1	90	⁸² Se	NEMO-3	¹ ARNOLD	18
< 1.8–22	90	< 1.6–21	90	^{116}Cd	AURORA	² BARABASH	18
< 0.9–1.3	90	< 0.5–0.8	90	¹⁰⁰ Mo	NEMO-3	³ ARNOLD	14
<120	90			¹⁰⁰ Mo	$0^+ \rightarrow 2^+$	⁴ ARNOLD	07
0.692 + 0.050 - 0.050	8 68	$0.305 + 0.026 \\ - 0.025$	68	^{76}Ge	Enriched HPGe	⁵ KLAPDOR-K	. 06 A
< 2.5	90	0.020		¹⁰⁰ Mo	0ν , NEMO-3	⁶ ARNOLD	05A
< 3.8	90			^{82}Se	0ν , NEMO-3	⁷ ARNOLD	05A
< 1.5 - 2.0	90			¹⁰⁰ Mo	0ν , NEMO-3	⁸ ARNOLD	04
< 3.2–3.8	90			⁸² Se	0ν , NEMO-3	⁹ ARNOLD	04
< 1.6-2.4	90	< 0.9–5.3	90	¹³⁰ Te	Cryog. det.	¹⁰ ARNABOLDI	03
< 2.2	90	<2.5	90	^{116}Cd	¹¹⁶ CdWO ₄ scint.	¹¹ DANEVICH	03
< 3.2–4.7	90	< 2.4–2.7	90	¹⁰⁰ Mo	ELEGANT V	¹² EJIRI	01
< 1.1	90	<0.64	90	76 Ge	Enriched HPGe	¹³ GUENTHER	97
< 4.4	90	<2.3	90	¹³⁶ Xe	ТРС	¹⁴ VUILLEUMIER	93
		<5.3		¹²⁸ Te	Geochem	¹⁵ BERNATOW	92

¹ ARNOLD 18 use the NEMO03 tracking detector, with 0.93 kg of ⁸²Se mass and 5.25 y exposure to obtain the limits for the hypothetical right-handed currents. Supersedes ARNOLD 05A.

- ² BARABASH 18 use 1.162 kg of ¹¹⁶CdWO₄ scintillating crystals to obtain this limits for the hypothetical right-handed currents in the $0\nu\beta\beta$ decay of ¹¹⁶Cd.
- ³ARNOLD 14 is based on 34.7 kg yr of exposure of the NEMO-3 tracking calorimeter. The reported range limit on $\langle \lambda \rangle$ and $\langle \eta \rangle$ reflects the nuclear matrix element uncertainty in ¹⁰⁰Mo.
- ⁴ ARNOLD 07 use NEMO-3 half life limit for 0ν -decay of ¹⁰⁰Mo to the first excited 2⁺state of daughter nucleus to limit the right-right handed admixture of weak currents $\langle \lambda \rangle$. This limit is not competitive when compared to the decay to the ground state.
- ⁵ Re-analysis of data originally published in KLAPDOR-KLEINGROTHAUS 04A. Modified pulse shape analysis leads the authors to claim 6σ statistical evidence for observation of 0ν -decay. Authors use matrix element of MUTO 89 to determine $\langle \lambda \rangle$ and $\langle \eta \rangle$. Uncertainty of nuclear matrix element is not reflected in stated errors.
- ⁶ ARNOLD 05A derive limit for $\langle \lambda \rangle$ based on ¹⁰⁰Mo data collected with NEMO-3 detector. No limit for $\langle \eta \rangle$ is given. Supersedes ARNOLD 04.

⁷ ARNOLD 05A derive limit for $\langle \lambda \rangle$ based on ⁸²Se data collected with NEMO-3 detector. No limit for $\langle \eta \rangle$ is given. Supersedes ARNOLD 04.

- ⁸ ARNOLD 04 use the matrix elements of SUHONEN 94 to obtain a limit for $\langle \lambda \rangle$, no limit for $\langle \eta \rangle$ is given. This limit is more stringent than the limit in EJIRI 01 for the same nucleus. ⁹ ARNOLD 04 use the matrix elements of TOMODA 91 and SUHONEN 91 to obtain a
- ⁹ ARNOLD 04 use the matrix elements of TOMODA 91 and SUHONEN 91 to obtain a limit for $\langle \lambda \rangle$, no limit for $\langle \eta \rangle$ is given.
- ¹⁰ Supersedes ALESSANDRELLO 00. Cryogenic calorimeter search. Reported a range reflecting uncertainty in nuclear matrix element calculations.
- ¹¹Limits for $\langle \lambda \rangle$ and $\langle \eta \rangle$ are based on nuclear matrix elements of STAUDT 90. Supersedes DANEVICH 00.
- ¹² The range of the reported $\langle \lambda \rangle$ and $\langle \eta \rangle$ values reflects the spread of the nuclear matrix elements. On axis value assuming $\langle m_{\nu} \rangle = 0$ and $\langle \lambda \rangle = \langle \eta \rangle = 0$, respectively.
- 13 GUENTHER 97 limits use the matrix elements of STAUDT 90. Supersedes BALYSH 95 , and BALYSH 92.
- 14 VUILLEUMIER 93 uses the matrix elements of MUTO 89. Based on a half-life limit 2.6×10^{23} y at 90%CL.
- ¹⁵ BERNATOWICZ 92 takes the measured geochemical decay width as a limit on the 0ν width, and uses the SUHONEN 91 coefficients to obtain the least restrictive limit on η . Further details of the experiment are given in BERNATOWICZ 93.

Double- β Decay REFERENCES

ABE	23	PRL 130 051801	S. Abe <i>et al.</i>	(KamLAND-Zen Collab.)
ADAMS	23A	PRL 131 249902 (errat		(CUORE Collab.)
AGOSTINI	23	PRL 131 142501	M. Agostini <i>et al.</i>	(GERDA Collab.)
AGUERRE	23	EPJ C83 1117	X. Aguerre <i>et al.</i>	(NEMO-3 Collab.)
ARNQUIST	23	PRL 130 062501	I.J. Arnquist <i>et al.</i>	(MAJORANA Collab.)
AUGIER	23	PR C107 025503	C. Augier <i>et al.</i>	(CUPID-Mo Collab.)
AUGIER	23A	PRL 131 162501	C. Augier <i>et al.</i>	(CUPID-Mo Collab.)
AZZOLINI	23A	PRL 131 222501	O. Azzolini <i>et al.</i>	(CUPID-0 Collab.)
NOVELLA	23	JHEP 2309 190	P. Novella <i>et al.</i>	(NEXT Collab.)
ADAMS	22A	NAT 604 53	D.Q. Adams <i>et al.</i>	(CUORE Collab.)
ADAMS	22B	PRL 129 222501	D.Q. Adams <i>et al.</i>	(CUORE Collab.)
APRILE	22A	PR C106 024328	E. Aprile <i>et al.</i>	(XENON1T Collab.)
APRILE	22B	PRL 129 161805	E. Aprile <i>et al.</i>	(XENONnT Collab.)
AUGIER	22	EPJ C82 1033	C. Augier <i>et al.</i>	(CUPID-Mo Collab.)
AZZOLINI	22	PRL 129 111801	O. Azzolini <i>et al.</i>	(CUPID-0 Collab.)
NOVELLA	22	PR C105 055501	P. Novella <i>et al.</i>	(NEXT Collab.)
ADAMS	21	PRL 126 171801	D.Q. Adams <i>et al.</i>	(CUORE Collab.)
Also	21	PRL 131 249902 (errat		(CUORE Collab.)
ADAMS	21A	EPJ C81 567	D.Q. Adams <i>et al.</i>	(CUORE Collab.)
ARMENGAUD	21	PRL 126 181802	E. Armengaud et al.	(CUPID-Mo Collab.)
ARNQUIST	21	PR C103 015501	I.J. Arnquist et al.	(MAJORANA Collab.)
ADAMS	20A	PRL 124 122501	D.Q. Adams <i>et al.</i>	(CUORE Collab.)
AGOSTINI	20B	PRL 125 252502	M. Agostini <i>et al.</i>	(GERDA Collab.)
ARMENGAUD	20	EPJ C80 674	E. Armengaud <i>et al.</i>	(CUPID-Mo Collab.)
AGOSTINI	19	SCI 365 1445	M. Agostini <i>et al.</i>	(GERDA Collab.)
ALDUINO	19	EPJ C79 795	C. Alduino <i>et al.</i>	(CUORE Collab.)
ALENKOV	19	EPJ C79 791	V. Alenkov <i>et al.</i>	(AMoRE Collab.)
ANTON	19	PRL 123 161802	G. Anton <i>et al.</i>	(ÈXO-200 Collab.)
APRILE	19E	NAT 568 532	E. Aprile <i>et al.</i>	(XENON1T Collab.)
ARNOLD	19	EPJ C79 440	R. Arnold <i>et al.</i>	(NEMO-3 Collab.)
AZZOLINI	19	PRL 123 032501	O. Azzolini <i>et al.</i>	(CUPID-0 Collab.)
AZZOLINI	19B	PRL 123 262501	O. Azzolini <i>et al.</i>	(CUPID-0 Collab.)
NI	19	CP C43 113001	K. Ni <i>et al.</i>	(PandaX-II Collab.)
ALBERT	18	PRL 120 072701	J.B. Albert <i>et al.</i>	(EXO-200 Collab.)
ALDUINO	18	PRL 120 132501	C. Alduino <i>et al.</i>	(CUORE Collab.)
ARNOLD	18	EPJ C78 821	R. Arnold <i>et al.</i>	(NEMO-3 Collab.)
BARABASH	18	PR D98 092007	A.S. Barabash <i>et al.</i>	(AURORA Collab.)
ALBERT	17C	PR D96 092001	J.B. Albert <i>et al.</i>	(EXO-200 Collab.)
ALDUINO	17	EPJ C77 13	C. Alduino <i>et al.</i>	(CUORE Collab.)
ARNOLD	17	PR D95 012007	R. Arnold <i>et al.</i>	(NEMO-3 Collab.)
ALDUINO	16	PR C93 045503	C. Alduino <i>et al.</i>	(CUORE Collab.)
ARNOLD	16	PR D93 112008	R. Arnold <i>et al.</i>	(NEMO-3 Collab.)
ARNOLD	16A	PR D94 072003	R. Arnold <i>et al.</i>	(NEMO-3 Collab.)
ASAKURA	16	NP A946 171	K. Asakura <i>et al.</i>	(KamLAND-Zen Collab.)

https://pdg.lbl.gov

Page 15

Created: 5/31/2024 10:16

AGOSTINI	15A	EPJ C75 416	M. Agostini <i>et al.</i>	(GERDA Collab.)
ALFONSO	15	PRL 115 102502	K. Alfonso <i>et al.</i>	(CUORE Collab.)
ARNOLD	15	PR D92 072011	R. Arnold <i>et al.</i>	(ŇEMO-3 Collab.)
ALBERT	14	PR C89 015502	J. Albert <i>et al.</i>	(EXO-200 Collab.)
ALBERT	14B	NAT 510 229	J.B. Albert <i>et al.</i>	(EXO-200 Collab.)
ARNOLD	14	PR D89 111101	R. Arnold et al.	(NEMO-3 Collab.)
GAVRILYAK	13	PR C87 035501	Yu.M. Gavrilyuk et al.	(
ANDREOTTI	12	PR C85 045503	E. Andreotti <i>et al.</i>	(CUORICINO Collab.)
GANDO	12A	PR C85 045504	A. Gando <i>et al.</i>	(KamLAND-Zen Collab.)
ACKERMAN	11	PRL 107 212501	N. Ackerman <i>et al.</i>	(EXO Collab.)
ARNOLD	11	PRL 107 062504	R. Arnold <i>et al.</i>	(NEMO-3 Collab.)
BARABASH	11A	PAN 74 312	A.S. Barabash <i>et al.</i>	(NEMO-3 Collab.)
DANADASH	117	Translated from YAF 74		(NEWIO-5 CONAD.)
ARGYRIADES	10	NP A847 168	J. Argyriades <i>et al.</i>	(NEMO-3 Collab.)
BELLI	10	NP A846 143	P. Belli <i>et al.</i>	(DAMA-INR Collab.)
ARGYRIADES	09	PR C80 032501	J. Argyriades <i>et al.</i>	(NEMO-3 Collab.)
KIDD	09	NP A821 251	M. Kidd <i>et al.</i>	(NEWIO-5 CONAD.)
UMEHARA	09	PR C78 058501	S. Umehara <i>et al.</i>	
ARNOLD	08	NP A781 209	R. Arnold <i>et al.</i>	(NEMO 2 Collab)
KLAPDOR-K		MPL A21 1547		(NEMO-3 Collab.)
-			H.V. Klapdor-Kleingrothaus,	
ARNOLD	05A	PRL 95 182302	R. Arnold <i>et al.</i>	(NEMO-3 Collab.)
AALSETH	04	PR D70 078302	C.E. Aalseth <i>et al.</i>	
ARNOLD	04	JETPL 80 377	R. Arnold <i>et al.</i>	(NEMO-3 Collab.)
	044	Translated from ZETFP		
KLAPDOR-K	-	PL B586 198	H.V. Klapdor-Kleingrothaus	
KLAPDOR-K		PR D70 078301	H.V. Klapdor-Kleingrothaus,	A. Dietz, I.V. Krivosheina
OGAWA	04	NP A730 215	I. Ogawa <i>et al.</i>	
ARNABOLDI	03	PL B557 167	C. Arnaboldi <i>et al.</i>	
DANEVICH	03	PR C68 035501	F.A. Danevich <i>et al.</i>	
AALSETH	02B	PR D65 092007	C.E. Aalseth <i>et al.</i>	(IGEX Collab.)
DEBRAECKEL		PRL 86 3510	L. De Braeckeleer <i>et al.</i>	
EJIRI	01	PR C63 065501	H. Ejiri <i>et al.</i>	
KLAPDOR-K	01	EPJ A12 147	H.V. Klapdor-Kleingrothaus	et al.
KLAPDOR-K	01B	MPL A16 2409	H.V. Klapdor-Kleingrothaus	et al.
ALESSAND	00	PL B486 13	A. Alessandrello <i>et al.</i>	
DANEVICH	00	PR C62 045501	F.A. Danevich <i>et al.</i>	
ARNOLD	99	NP A658 299	R. Arnold <i>et al.</i>	(NEMO Collab.)
GUENTHER	97	PR D55 54	M. Gunther <i>et al.</i>	(Heidelberg-Moscow Collab.)
ARNOLD	96	ZPHY C72 239	R. Arnold <i>et al.</i>	(BCEN, CAEN, JINR+)
BALYSH	95	PL B356 450	A. Balysh <i>et al.</i>	(Heidelberg-Moscow Collab.)
DASSIE	95	PR D51 2090	D. Dassie <i>et al.</i>	(NEMO Collab.)
EJIRI	95	JPSJ 64 339	H. Ejiri <i>et al.</i>	(OSAK, KIEV)
SUHONEN	94	PR C49 3055	J. Suhonen, O. Civitarese	
BERNATOW	• •	PR C47 806	T. Bernatowicz <i>et al.</i>	
VUILLEUMIER		PR D48 1009	J.C. Vuilleumier <i>et al.</i>	(WUSL, TATA)
	93 92			(NEUC, CIT, VILL)
BALYSH		PL B283 32	A. Balysh <i>et al.</i> T. Barrataviat <i>et al.</i>	(MPIK, KIAE, SASSO)
BERNATOW		PRL 69 2341	T. Bernatowicz <i>et al.</i>	(WUSL, TATA)
SUHONEN	91 01	NP A535 509	J. Suhonen, S.B. Khadkikar	, A. Faessler (JYV+)
TOMODA	91	RPP 54 53	T. Tomoda	
STAUDT	90	EPL 13 31	A. Staudt, K. Muto, H.V. I	
мито	89	ZPHY A334 187	K. Muto, E. Bender, H.V.	Klapdor (TINT, MPIK)